frontiers | Frontiers in Marine Science

TYPE Original Research
PUBLISHED 23 March 2023
DOI 10.3389/fmars.2023.1118795

Check for updates

OPEN ACCESS

EDITED BY
Sha Lou,
Tongji University, China

REVIEWED BY
Guoxiang Wu,
Ocean University of China, China
Jishang Xu,
Ocean University of China, China

*CORRESPONDENCE
Chunyan Zhou
cyzhou@hhu.edu.cn

SPECIALTY SECTION
This article was submitted to Coastal Ocean Processes, a section of the journal Frontiers in Marine Science

RECEIVED 08 December 2022
ACCEPTED 13 March 2023
PUBLISHED 23 March 2023

CITATION
Wu Z, Zhou C, Wang P and Fei Z (2023) Responses of tidal dynamic and water exchange capacity to coastline change in the Bohai Sea, China.
Front. Mar. Sci. 10:1118795.
doi: 10.3389/fmars.2023.1118795

COPYRIGHT
© 2023 Wu, Zhou, Wang and Fei. This is an open-access article distributed under the terms of the Creative Commons Attribution License (CC BY). The use, distribution or reproduction in other forums is permitted, provided the original author(s) and the copyright owner(s) are credited and that the original publication in this journal is cited, in accordance with accepted academic practice. No use, distribution or reproduction is permitted which does not comply with these terms.

Responses of tidal dynamic and water exchange capacity to coastline change in the Bohai Sea, China

Zhengcheng Wu[1], Chunyan Zhou[1*], Peng Wang[2] and Zihao Fei[1]

[1]College of Harbour, Coastal and Offshore Engineering, Hohai University, Nanjing, China, [2]Marine Academy of Zhejiang Province, Hangzhou, China

Bohai Sea (BHS) is a semi-enclosed shallow continental sea in China that has suffered from the deteriorative hydrodynamic environment due to large-scale reclamation. Single-factor simulations of tidal dynamic and material transport under the influence of the coastline changes from 1999 to 2019 in BHS were carried out. The model results showed that the amplitude of M2 tide increased slightly in Liaodong Bay and Bohai Bay, but decreased obviously in Laizhou Bay along with larger reclamation. The amplitude variation of the semi-diurnal constituents (M2, S2) was greater than the diurnal ones (K1, O1). The basin residence time in Liaodong Bay and Laizhou Bay increased by 5.44% and 49.44% from 1999 to 2019, respectively. Runoff of the Huanghe River can shorten the residence time of Laizhou bay while only having little effect on Bohai Bay and Liaodong Bay. The study of the Bohai Sea evolution can provide recommendations for subsequent marine ecological restoration efforts and serve as a reference for the study of other large semi-enclosed bays.

KEYWORDS

Bohai Sea, coastline change, tidal dynamics, tidal prism, land reclamation, water-exchange

1 Introduction

Reclamation changes the coastline and geomorphology of coastal areas and has an obvious impact on the propagation, refraction, reflection and dissipation of bottom energy of gravity waves such as tidal waves and storm surges, thus changing the phase of ocean wave fluctuations and the spatial distribution of energy (Zhu et al., 2016). Large-scale reclamation has alleviated the problem of conflicting urban land use, but the water environment in many bays has suffered some negative effects due to some unregulated engineering construction (Li et al., 2020).

Many researchers have analyzed the water environment changes of bays due to human activities. The construction of sea walls in the Mokpo coastal zone has resulted in a decrease of 43 cm for the extreme low tide and an increase of 60 cm for the extreme high tide. This amplification can cause severe inundation when a typhoon hits (Kang, 1999). Reclamation

significantly altered the morphological characteristics of the Shannon estuary, leading to changes in the physical and hydrodynamics environment of the estuary, and modification of the characteristics of the wetland habitat in the estuary environment (Healy and Hickey, 2002). Liang et al. (2018) investigated the hydro-morphodynamics of Caofeidian channel-shoal along with large-scale reclamation projects from 2003 to 2020. Numerical results indicated that continuous land reclamation caused a continuous loss of tidal sediment volume by reducing the sediment storage capacity of tidal flats.

Bohai Sea is a semi-enclosed shallow continental sea, located within 37°07′N-41°00′N, 117°35′E-121°10′E (Figure 1). The sea is divided into four parts: Bohai Bay, Liaodong Bay, Laizhou Bay and the central BHS. The sea covers an area of 77,000 km^2 with an average depth of 18 m, and 95% of BHS is less than 30 m.

Coastal areas were reclaimed along with rapid economic development in cities surrounding BHS. From 1987 to 2016, the total area of BHS decreased by 1889.51 km² and the length of the coastline increased by 1672.16 km (Zhu et al., 2018). The average reclamation rate in BHS is 325 km²/year, and more than 60% of the total reclamation area is unused land, aquaculture land and saline land (Ding et al., 2019). Zhao and Sun (2013) studied the impact of reclamation on the wave in the Caofeidian region and found that the significant wave height tends to decline by 0.1-0.4 m from 2000 to 2010. Li et al. (2010) used an integrated hydrodynamic-dispersion numerical model to investigate the impact of land reclamation on the water exchange in the coastal area of Tianjin in Bohai Bay. From 1976 to 2011, the tidal system in BHS changed significantly with M2 amplitudes varying up to 20 cm in some areas (Pelling et al., 2013). Jia et al. (2018) predicted the effects of shoreline changes in Bohai Bay and showed that the coastline change weakened the residual currents, resulting in weaker water exchange and poor pollutant-diffusing capacity.

However, there is still a lack of studies on the effects of water environmental degradation in the whole BHS due to reclamation, which is essential for providing a comprehensive reference for future ecological restoration. In this paper, single-factor simulations of the tidal dynamics are performed under the influence of coastline changes in BHS and compare the impact of runoff of the Huanghe River on the water exchange capacity in BHS before and after reclamation. This research explores the response of tidal prism, tidal system and water exchange to large-scale reclamation in BHS from 1999 to 2019, and provides a reference for similar studies of other large semi-enclosed bays with intensive anthropogenic activities.

2 Data and methods

2.1 Coastline data

The coastline was derived from the Chinese mainland shoreline (CLINE) database. The CLINE database consists of a coastline extraction algorithm based on the remote sensing image data from Google Earth Engine, 37 years (1984~2020) of the year-by-year coastline of China and its supporting analysis information. Compared with other coastline databases, the CLINE database has the characteristics of high temporal resolution, lengthy periods, and large spatial coverage for the coastline of mainland China. Reclamation projects in BHS were rare before 2000 and the Chinese government introduced strict control measures to prohibit reclamation in 2018, thereafter the coastline was almost

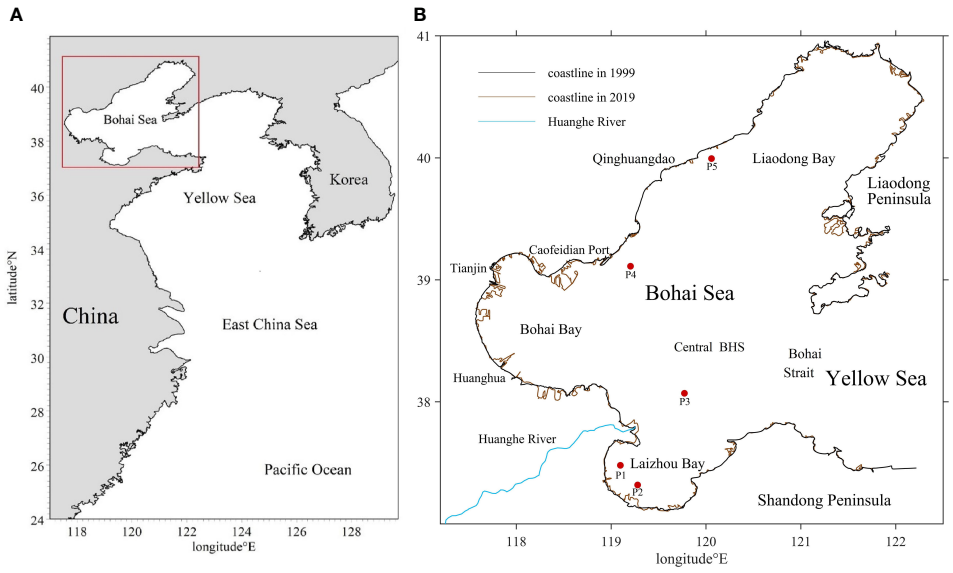

FIGURE 1
(A) Location of Bohai Sea; **(B)** Coastline in 1999 and 2019.

unchanged by human activities. This paper chose the coastline in 1999, 2009 and 2019 to build hydrodynamic models.

2.2 Numerical model

The simulations were performed using the MIKE 21 Flow Model. The momentum equations are the incompressible, Reynolds-averaged form of the Navier–Stokes equations, obeying the Boussinesq assumption and the hypothesis of vertical hydrostatic pressure. The continuity equation is Equation 1, two horizontal momentum equations for the x and y components are Equation 2 and Equation 3, respectively:

$$\frac{\partial h}{\partial t}+\frac{\partial h\bar{u}}{\partial x}+\frac{\partial h\bar{v}}{\partial y}=hS \tag{1}$$

$$\frac{\partial h\bar{u}}{\partial t}+\frac{\partial h\bar{u}^2}{\partial x}+\frac{\partial h\bar{v}\bar{u}}{\partial y}=f\bar{v}h-gh\frac{\partial \eta}{\partial x}-\frac{\tau_{bx}}{\rho_0}$$

$$\frac{1}{\rho_0}\left(\frac{\partial S_{xx}}{\partial x}+\frac{\partial S_{xy}}{\partial y}\right)+\frac{\partial}{\partial x}(hT_{xx})+\frac{\partial}{\partial y}(hT_{xy})+hu_sS \tag{2}$$

$$\frac{\partial h\bar{v}}{\partial t}+\frac{\partial h\overline{uv}}{\partial x}+\frac{\partial h\bar{v}^2}{\partial y}=-f\bar{u}h-gh\frac{\partial \eta}{\partial y}-\frac{\tau_{by}}{\rho_0}-$$

$$\frac{1}{\rho_0}\left(\frac{\partial S_{yx}}{\partial x}+\frac{\partial S_{yy}}{\partial y}\right)+\frac{\partial}{\partial x}(hT_{xy})+\frac{\partial}{\partial y}(hT_{yy})+hv_sS \tag{3}$$

where h is the total water depth, t time, x and y are the Cartesian coordinates, and are depth averages of velocity components in the x and y direction, S is the magnitude of the discharge because of point sources, f is the Coriolis parameter, g is gravitational acceleration, η is surface elevation, ρ_0 is the reference density of water, $\tau_{bx}$and τ_{by} are the components of bottom stress, u_s, v_s are the velocity at which the water is discharged into the ambient water, T_{xy}, T_{xx} and T_{yy} are the lateral stresses.

A transport module was coupled to the Mike21 hydrodynamic model to simulate tracer transport, as Equation 4 and Equation 5 (Bai et al., 2021).

$$\frac{\partial (hC)}{\partial t}+\frac{\partial (\bar{u}hC)}{\partial x}+\frac{\partial (\bar{v}hC)}{\partial y}$$
$$=\frac{\partial}{\partial x}\left(hD_x\frac{\partial C}{\partial x}\right)+\frac{\partial}{\partial y}\left(hD_y\frac{\partial C}{\partial y}\right)-FhC+S \tag{4}$$

$$S=Q_s(C_s-C) \tag{5}$$

where D_x, D_y are the diffusion coefficients in the x and y directions, C is the composite concentration, F is the linear attenuation coefficient, S is the source discharge, Q_s is source-sink term flow, C_s is the concentration at the source-sink.

The open boundary conditions are water levels derived from tide prediction based on the harmonic constants of tide stations at the open boundary. The bottom friction is one of the main factors affecting the calculation accuracy, which is set as a constant Chezy number of 118 after model validation.

2.3 Residence time calculation

Residence time is calculated by the Eulerian definition. A tracer with a concentration of 1 is released in the bay, and the concentration of each grid cell changes under the combined effect of runoff and water exchange outside the bay, and the volume changes with the rise and fall of the tide level. The relative tracer mass (RTM) is given as Equation 6 (Yuan et al., 2021):

$$RTM(t)=\frac{\sum_{i=1}^{n}C_i(t)V_i(t)}{\sum_{i=1}^{n}C_i(t_0)V_i(t_0)} \tag{6}$$

where the subscript i is the number of the grid, C_i is the concentration of grid number i at the time t, V_i is the volume of grid number i at the time t. Due to the initial condition setting, here $C_i(t_0)$=1, so the denominator of Equation 6 is the initial bay volume.

Residence time is the average time that a dissolved or suspended material resides in the bay before it is transported into the open sea (Liu et al., 2011). Basin residence time and local residence time are used to reflect the water exchange capacity of the whole bay and a single grid respectively. The residence time in Zhao et al. (2002) was defined as the time required for the concentration of the passive tracer in a given region to decay to e^{-1} (37%) of the initial value. In this paper, the basin residence time is the moment when the RTM $=e^{-1}$ (37%) after a polynomial fit of the average bay concentration (Figure 2). This calculation method eliminates the effect of tidal action on the variation of the average concentration in the bay by polynomial fitting, thus accurately reflecting the residence time in the bay.

But this method cannot be used to calculate the local residence time. Polynomial fit for each grid is too computationally intensive and the water level of the nearshore area drops substantially at low tide, which will cause a decrease in the number of tracers contained in the grid with decreasing water depth, resulting in a small local residence time. Therefore, the residence time of the grid is the moment when the current concentration of the grid is for the first time less than 37% of the initial concentration.

2.4 Tidal prism calculation

The tidal prism is an essential parameter reflecting the hydrodynamics and water environment of a bay, which is highly

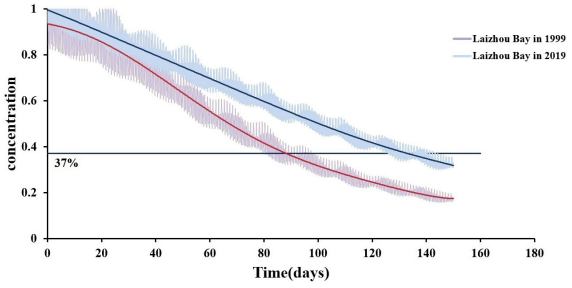

FIGURE 2
Time series of concentration and the polynomial fit in Laizhou Bay.

related to the residence time (Ying et al., 2018). The reduction of the tidal prism will decrease the intensity of water exchange between the bay and the outer sea, and slow down the migration and diffusion of pollutants, thus affecting the self-purification ability of the bay (Fang et al., 2015).

The tidal prism is calculated as the flux of seawater through the boundary section during a high or low tide cycle, and the average of the seawater fluxes in a high tide and low tide period is taken as the tidal prism for the whole tidal cycle. According to this definition, the tidal prism Q is given by:

$$Q = \int_{t_1}^{t_2} (Q_u + Q_v) dt \tag{7}$$

where Q_u and Q_v are the tidal flux through the section per unit time in the x and y directions, t_1 and t_2 are the start and end times of the high tide cycle or low tide cycle, respectively.

2.5 Eulerian tidal residual current calculation

The nonlinear action of tidal currents generates tidal residual currents, thus forming tidal circulation. Although the tidal circulation is relatively weak, the tidal residual current plays an important role in the migration and long-term stable distribution of pollutants in the sea because the Bohai Sea is semi-enclosed and the tide is the main dynamic factor in BHS. Eulerian tidal residual current is defined as the averaged speed at a fixed location during several tidal cycles and calculated according to Equation 8:

$$\begin{aligned} U_E &= \tfrac{1}{nT} \int_{t_0}^{t_0+nt} u(x_0, t) dt \\ V_E &= \frac{1}{nT} \int_{t_0}^{t_0+nt} v(x_0, t) dt \end{aligned} \tag{8}$$

where U_E and V_E are Eulerian average velocities in x and y directions respectively, t_0 is the initial moment of calculation, T is the tidal period, $u(x_0, t)$, $v(x_0, t)$ is the velocity of a fixed point in the x and y directions, n is the number of calculation periods, $N=nT/\Delta t$, Δt is the time step of the numerical simulation. In this paper, the 60 tidal cycles were counted in order to calculate the Eulerian tidal residual current, starting at the highest tidal level of the spring tide and ending at the highest tidal level of the spring tide a month later.

2.6 Model validation

The measured tidal level and current from five stations shown in Figure 1B were used for model validation. Figure 3 shows that the simulated tide levels are in very good match with the observation data. It is shown in Figure 4 that the modeled results of tidal velocity and direction have the same variation pattern with the observation data.

To quantitatively evaluate the accuracy of the hydrodynamic model simulation results, using the statistical method proposed by Willmott (1981) and correlation coefficient (CC) to evaluate simulation results:

$$skill = 1 - \frac{\sum_{i=1}^{N} |X_m - X_s|^2}{\sum_{i=1}^{N} (|X_m - \overline{X_s}| + |X_s - \overline{X_s}|)^2} \tag{9}$$

$$\mathrm{CC} = \frac{\sum (X_s - \overline{X_s})(X_m - \overline{X_m})}{[\sum (X_s - \overline{X_s})^2 \sum (X_m - \overline{X_m})^2]^{1/2}} \tag{10}$$

where X_m is the measured value, X_s is the simulated value, $\overline{X_m}$ and $\overline{X_s}$ are the mean value of the simulated and the measured value, respectively.

The skill value obtained from Equation 9 represents the simulated value deviation from the average of measured values and the CC represents the correlation of two statistical variables, when skill > 0.65 and CC>0.80, it means that the model fits well. The simulated accuracy of tidal currents and tidal level at each observation station can be represented by the skill value and the CC value, as shown in Table 1.

The skill values are larger than 0.95 for the tidal level, while larger than 0.85 for the current speed and direction. The CC is larger than 0.90 for the tidal level, while larger than 0.80 for the current speed and direction, thus the model can reflect the hydrodynamic situation of the whole Bohai Sea.

3 Results and discussion

3.1 Tidal wave

Tidal movement is the most important form of seawater movement in BHS, and the main tides in BHS are O1, K1, M2 and S2, of which the dominant tide is M2. To analyze the changes in the tidal wave system, the same boundary conditions were applied, but with different coastlines in 1999 and 2019, respectively. The simulation results were analyzed by Tide Analysis of Height in Mike21 Toolbox to obtain the amplitude and phase of M2, K1, S2 and O1. The simulation results show that various patterns of semi-diurnal constituents M2 and S2 are similar, but the amplitude of M2 is much larger than that of S2. Diurnal constituents of K1 and O1 have similar variation patterns and amplitudes.

From 1999 to 2019, amplitude of M2 in BHS has changed by -0.222m to 0.760m. It increased slightly in Liaodong Bay and Bohai Bay and decreased obviously in Laizhou Bay with a maximum value of 0.22m. Compared with the other two bays, only the amplitude of the M2 tide in Laizhou Bay was decreased. The reduction of amplitude is most obvious in the western part of Laizhou Bay, and the reduction in some areas is more than 0.04m (Figure 5). The area with a variation of -0.05m to 0.05m accounts for 95.26% of the total area of BHS. The amplitude of diurnal constituents in BHS changed slightly, and the amplitude of K1 changed by -0.023m to 0.243m. The area with the variation of -0.01m to 0.01m accounts for 99.6% of the total area of BHS. The area with decreasing M2 amplitude is larger than the area with increasing amplitude, while the contrary is the case for K1. Overall, the amplitude change range of semi-diurnal constituents was larger than the diurnal ones. The phase change of M2 in Bohai Bay slowed, causing the tidal wave entering from the east to decelerate more slowly, and the phase of M2 in Liaodong Bay barely changed from 1999 to 2019. The cotidal

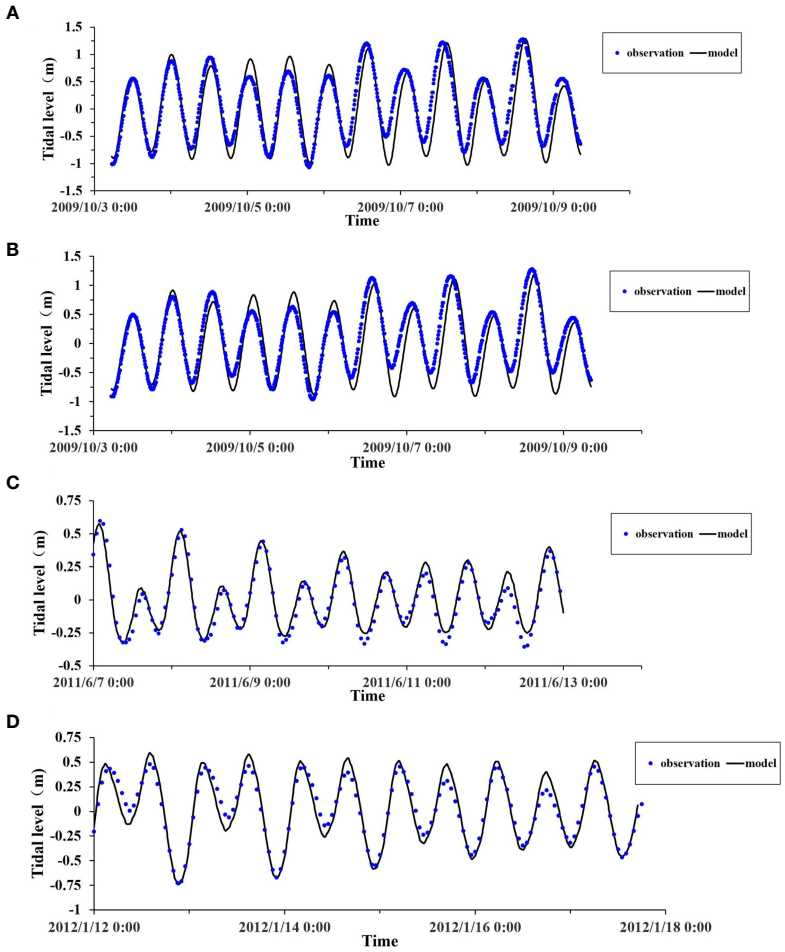

FIGURE 3
Tidal level comparison between model results and measured data at **(A)** Station P_1, **(B)** Station P_2, **(C)** Station P_3, **(D)** Station P_4.

line of K1 in most areas of BHS was deflected counterclockwise, resulting in a slight advance of tide time.

The Yellow River delta is characterized by high sediment load, fast accretion and frequent avulsions. To investigate the influence of the Yellow River Delta evolution on the tidal changes of Laizhou Bay, a case with shoreline only changes near the Yellow River Delta and remain unchanged at other areas was carried out. The results show that the amplitude changes are significant only in the vicinity of the Yellow River Delta, while less than 0.005 m for M2 and less than 0.002 m for K1 in most areas of Laizhou Bay. Therefore, the evolution of the Yellow River Delta is not the dominating factor contributing to tidal changes in the Laizhou Bay (Figures 6A, B).

Figures 6C, D shows that the amphidromic point of M2 near Qinhuangdao migrated 7.73km southwestward, and the amphidromic point near the Huanghe River estuary migrated 9.15 km southeastward. The amphidromic point of K1 in the Bohai Strait migrated 3.71 km southeastward. From the perspective of tidal energy distribution, tidal flats store tidal energy including potential tidal energy and kinetic energy during flood tides and release it during ebb tides. Tidal flats have two functions affecting tidal energy distribution: storage and dissipation. Compared with the tidal energy dissipation caused by bottom friction, the tidal energy storage in the mudflat area is much larger. (Song et al., 2013). The tidal energy stored in the mudflat area will be redistributed in the sea outside the mudflat area due to the reduction of the mudflat area caused by the reclamation, which resulted in the amphidromic point in BHS departing from the coastline (Zhu et al., 2016).

3.2 Residence time

Many seasonal rivers flow into BHS, with a total average annual runoff around 5.0×10^{10} m^3, more than a half comes from the Huanghe River (Ding et al., 2020). In this paper, the impact of the Huanghe River runoff on exchange was investigated in BHS, and the daily average flow of the Huanghe River was obtained from the Huanghe River Conservancy Commission of the Ministry of Water Resources. The simulation duration of Laizhou Bay, Bohai Bay and Liaodong Bay was 5 months, 30 months and 70 months respectively. Hydrodynamic models coupled with the transport module were established for Laizhou Bay and Bohai Bay with and without runoff from the Huanghe River in 1999 and 2019. Liaodong Bay is far away from the Huanghe River estuary, so the influence of

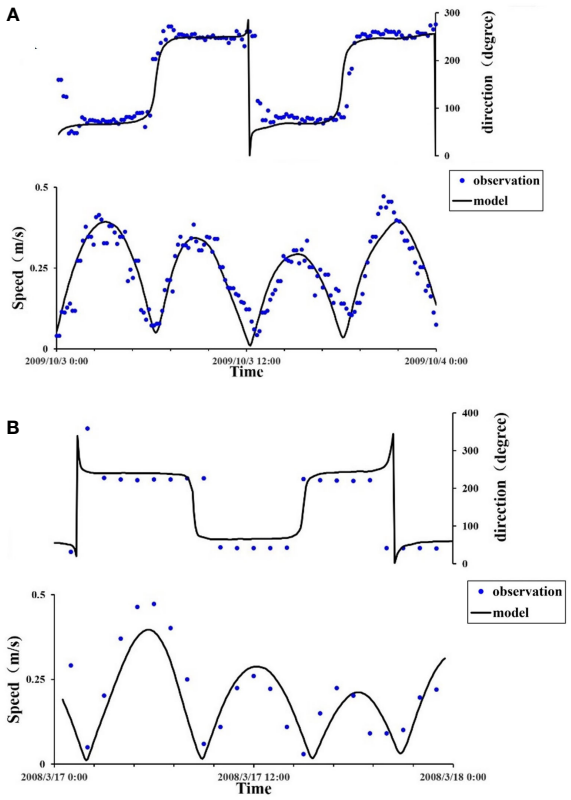

FIGURE 4
Current speed comparison between model results and measured data at **(A)** Station P_2, **(B)** Station P_5.

the Huanghe River runoff on the water exchange in Liaodong Bay was not considered here.

The results showed that the coastline change increased the basin residence time and local residence time in Laizhou Bay, especially in the nearshore waters (Figures 7A1, A3). Basin residence time in Laizhou Bay increased from 89 days in 1999 to 133 days in 2019 and the area with local residence time larger than 140 days increased significantly without considering runoff. Basin residence time in Bohai Bay increased from 466 days in 1999 to 510 days in 2019. The local residence time in the region (a) in the northern part of Bohai Bay decreased from 1999 to 2019 (Figures 7 B1, B3), which was related to the existence of circulation in that area before the construction of Caofeidian Port, impeding the material transport in the northern part of Bohai Bay. After the construction of Caofeidain Port in 2019, the circulation disappeared and Eulerian tidal residual current velocity in the region (a) increased (Figures 8C, D), accelerating the exchange of tracers in the northern part of Bohai Bay with the outer sea, thus leading to a smaller local residence time in the region (a). The local residence time in region (b) in the southern part of Bohai Bay increased from 1999 to 2019 (Figures 7B1, B3), mainly because the Eulerian tidal residual current direction in 2019 obliqued to the north compared to that in 1999, reducing the ability of the tracer to exchange directly with the outer sea, which was probably related to the reclamation shoreward in the southern part of Bohai Bay. The basin residence time in Liaodong Bay is 1894 days in 1999 and 1997 days in 2019, only increase by 5%, which indicates that coastline changes only have little effect on material transport in Liaodong Bay.

Runoff could shorten the basin residence time in Laizhou Bay and Bohai Bay (Table 2). However, the local residence time barely changed in most regions of Bohai Bay and Laizhou Bay with/without the runoff (Figure 7). The main reason is that the calculation methods of basin residence time and local residence time are different as shown in Section 2.3. Under the influence of runoff, the local residence time of Laizhou Bay changed very little and the residence time of Laizhou Bay decreased by 11 days in 1999 and 9 days in 2019, respectively. It indicates that runoff can intensify the oscillation of tracer concentration in the bay with high and low tides, thus affecting the fitted calculated basin residence time. However, the effect of runoff on local residence time is limited to the vicinity of the Huanghe River estuary.

The Eulerian tidal residual current (Figure 8) showed that Laizhou Bay exchanged water with the outer sea through the eastern coast, and the Eulerian residual velocity in this area was relatively large. However, the Eulerian residual velocity at the junction of Bohai Bay and the central BHS was low, leading to seawater containing the tracer staying in the center after flowing out of the bay during the low tide cycle and flowing back into Bohai Bay during the next high tide, so the residence time in Bohai Bay was relatively longer, and the coastline change had a relatively minor impact on the water exchange.

TABLE 1 Skill and CC value at each station.

Items	location	skill	CC
Tidal level	P1	0.95	0.92
	P2	0.95	0.91
	P3	0.98	0.97
	P4	0.98	0.97
Current speed	P2	0.94	0.89
	P5	0.85	0.85
Current direction	P2	0.92	0.9
	P5	0.88	0.82

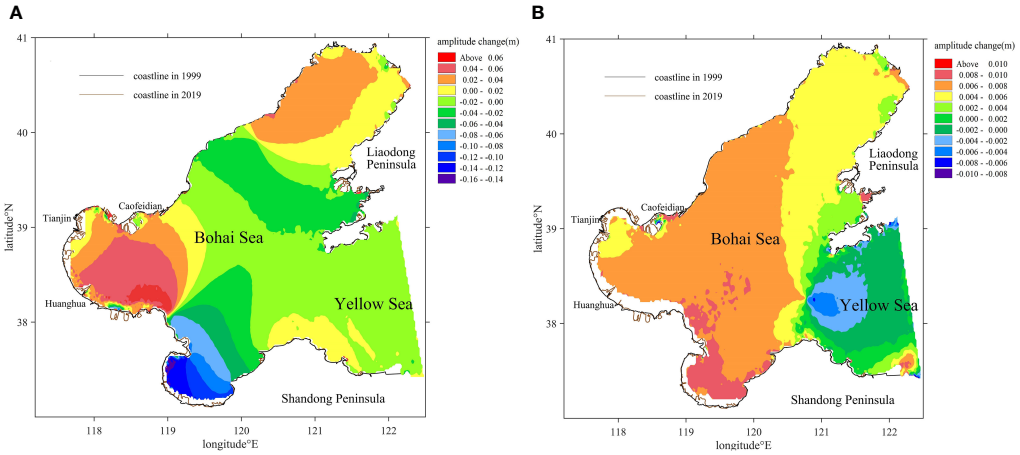

FIGURE 5
Tidal amplitude changes from 1999 to 2019 of **(A)** M2, **(B)** K1.

3.3 Tidal prism

To quantify the influence of the reclamation on the tidal prism of BHS and evaluate the impact of the reclamation on the water exchange capacity of the bay, hydrodynamic models were established to calculate the tidal fluxes in *x* and *y* directions at the boundary sections of three bays from June 1 to August 1. The average tidal prism of the three bays in BHS in 1999, 2009

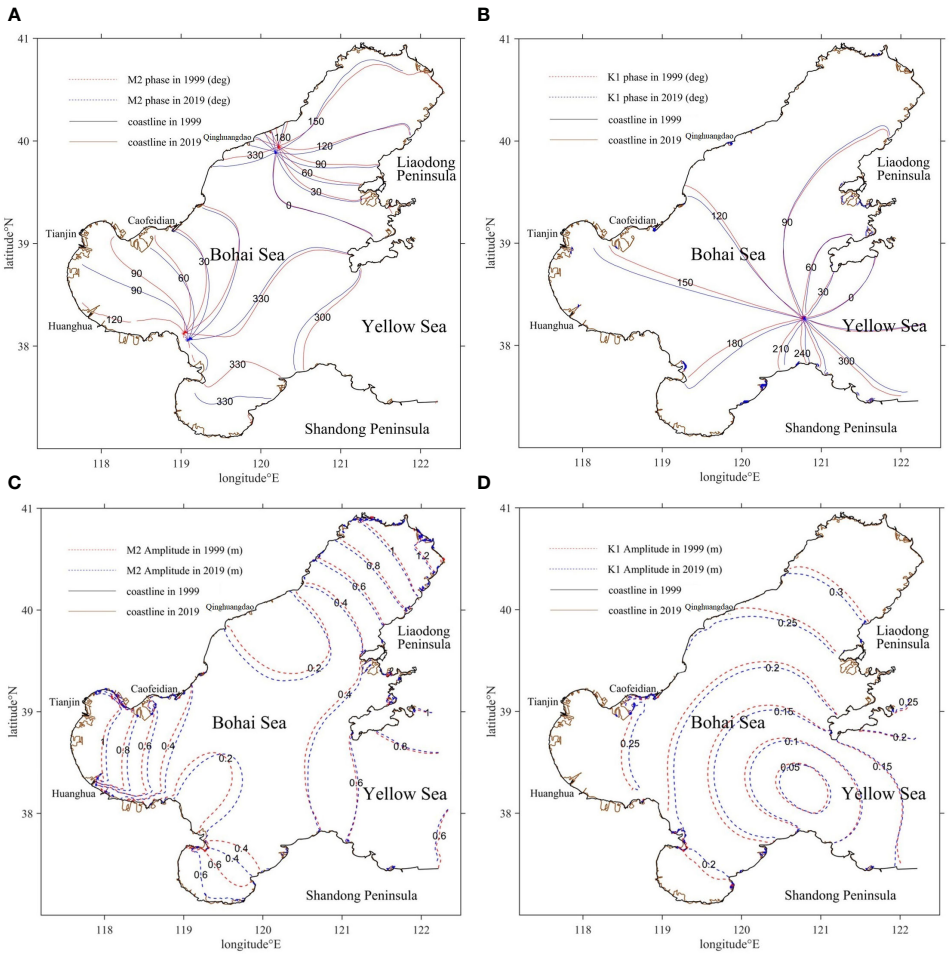

FIGURE 6
M2 and K1 tidal amplitudes and phases. **(A, B)** M2 and K1 tidal phases in 1999 and 2019. **(C, D)** M2 and K1 tidal amplitudes in 1999 and 2019.

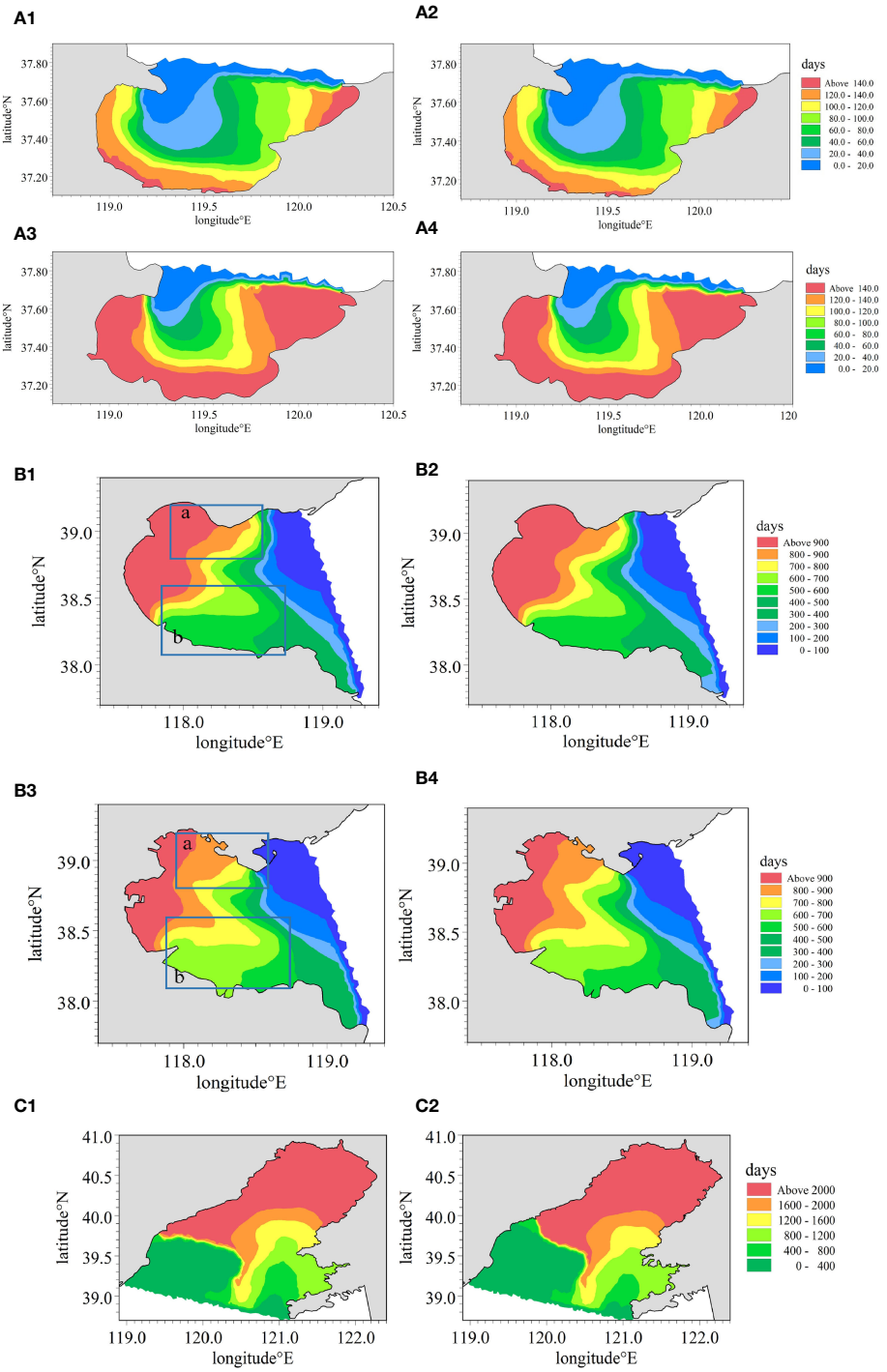

FIGURE 7
Local residence time **(A1)** Bohai Bay in 1999; **(A2)** Bohai Bay under the influence of with runoff in 1999; **(A3)** Bohai Bay in 2019; **(A4)** Bohai Bay with runoff in 2019; **(B1)** Laizhou Bay in 1999; **(B2)** Laizhou Bay with runoff in 1999; **(B3)** Laizhou Bay in 2019; **(B4)** Laizhou Bay with runoff in 2019; **(C1)** Liaodong Bay in 1999; **(C2)** Liaodong Bay in 2019.

and 2019 and its change rate relative to 1999 were listed in Table 3.

In general, the change of prism and residence time in Liaodong Bay was the smallest, and its area decrease was slightly smaller than the other two bays, which indicated that the coastline change in Liaodong Bay had the smallest influence on its water exchange capacity (Tables 2, 3). Therefore, it can be obtained that the water exchange capacity of bays with larger areas is less affected by coastline changes compared to bays with smaller areas. Laizhou Bay has a similar change rate of area with Bohai Bay, but Laizhou Bay has a larger decrease rate of tidal prism than Bohai Bay. The basin residence time increased by 58.97% and 10% respectively for Laizhou Bay and Bohai Bay from 1999 to 2019 without considering the runoff.

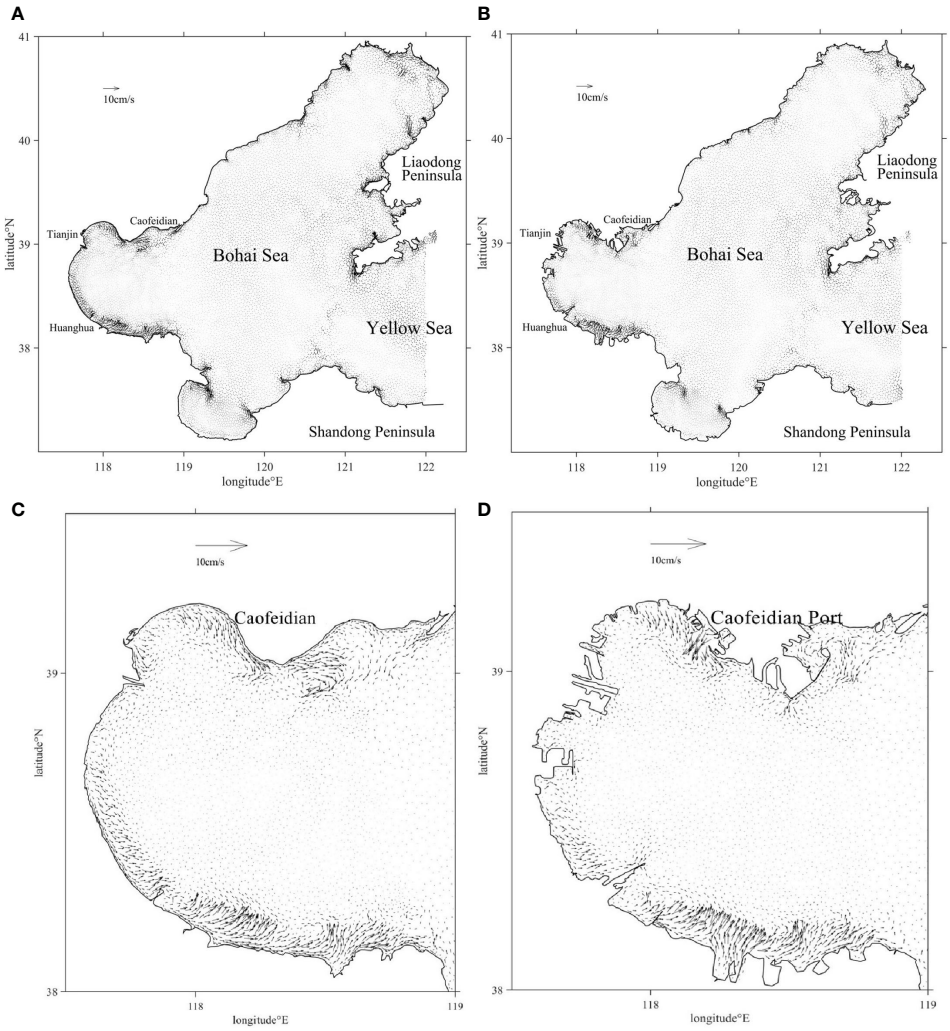

FIGURE 8
Simulated Eulerian tidal residual currents in **(A)** BHS in 1999; **(B)** BHS in 2019; **(C)** Bohai Bay in 1999; **(D)** Bohai Bay in 2019.

4 Conclusions

Large-scale of reclamation has a significant influence on the tidal regime and water exchange capacity in BHS. In this paper, coastline data of BHS in 1999, 2009, and 2019 were used to construct the hydrodynamic model. The model simulation data fit well with the measured data and can be used to study the effects of coastline changes on tidal currents and water exchange in BHS. The model results show that the amplitude of M2 increased slightly in Liaodong Bay and Bohai Bay, and decreased obviously in Laizhou Bay from 1999 to 2019. The amplitude variation of the semi-diurnal constituents (M2, S2) was greater than that of the diurnal ones (K1, O1). The amphidromic point of M2 near Qinhuangdao migrated 7.73km southwestward and the amphidromic point near the Huanghe River estuary migrated 9.15 km southeastward. The amphidromic point of K1 in the Bohai Strait migrated 3.71 km southeastward. Reclamation had weakened the water exchange capacity of BHS, and local residence time and basin residence time

TABLE 2 Basin residence time of the BHS with/without runoff in 1999 and 2019.

Bay	Basin residence time in 1999 with runoff(days) without runoff(days)	Basin residence time in 2019 with runoff(days) without runoff(days)
Laizhou Bay	89 78	133 124
Bohai Bay	466 460	510 506
Liaodong Bay	1894	1997

TABLE 3 Tidal prism and area of the BHS.

Bay	1999 Area(km^2) prism($\times10^{10}m^3$)	2019 Area(km^2) prism($\times10^{10}m^3$)	difference Area(%) prism(%)
Laizhou Bay	6155 0.719	5993 0.663	-2.63 -7.79
Bohai Bay	13179 2.077	12899 2.006	-2.12 -3.42
Liaodong Bay	35373 2.968	34649 2.938	-2.05 -1.01

in three bays had generally increased from 1999 to 2019. Some areas had different change trends due to changes in the Eulerian tidal residual current field. The circulation near Caofeidian Port disappeared with the construction of the port, leading to enhanced water exchange capacity in the northern part of Bohai Bay. With the influence of runoff, the local residence time in Laizhou Bay decreased by 11 days in 1999 and 9 days in 2019, respectively. Runoff only shortened the local residence time near the Huanghe River estuary and did not affect other areas. The research method can provide a reference for the study of other large semi-enclosed bays, and provide suggestions for subsequent marine ecological restoration efforts.

Data availability statement

Publicly available datasets were analyzed in this study. This data can be found here: http://www.coast-hhu.com/?page_id=2547.

Author contributions

ZW ran the numerical model, analyzed the results, and wrote the manuscript draft. CZ designed the numerical experiments and revised the manuscript. PW collected the coastline of BHS. ZF analyzed the coastline data. All authors contributed to the article and approved the submitted version.

Funding

National Natural Science Foundation of China (NSFC) 4160 6042, Fundamental Research Funds for the Central Universities B210202031.

Conflict of interest

The authors declare that the research was conducted in the absence of any commercial or financial relationships that could be construed as a potential conflict of interest.

Publisher's note

All claims expressed in this article are solely those of the authors and do not necessarily represent those of their affiliated organizations, or those of the publisher, the editors and the reviewers. Any product that may be evaluated in this article, or claim that may be made by its manufacturer, is not guaranteed or endorsed by the publisher.

References

Bai, T., Xu, J., Zhang, M., and Chang, C.-M. (2021). Seawater exchange rates for harbors based on the use of MIKE21 coupled with transport and particle tracking models. *J. Coast. Conserv.* 25 (2), 1–10. doi: 10.1007/s11852-021-00815-6

Ding, X., Guo, X., Zhang, C., Yao, X., Liu, S., Shi, J., et al. (2020). Water conservancy project on the huanghe river modifies the seasonal variation of chlorophyll-a in the bohai Sea. *Chemosphere.* 254, 126846. doi: 10.1016/j.chemosphere.2020.126846

Ding, X. S., Shan, X. J., Chen, Y. L., Jin, X. S., and Muhammed, F. R. (2019). Dynamics of shoreline and land reclamation from 1985 to 2015 in the bohai Sea, China. *J. Geographical Sci.* 29 (12), 2031–2046. doi: 10.1007/s11442-019-1703-1

Fang, S., Xie, Y., and Cui, L. (2015). "Analysis of tidal prism evolution and characteristics of the lingdingyang bay at pearl river estuary," in *MATEC Web of Conferences.* (EDP Sciences). 25, 01006. doi: 10.1051/matecconf/20152501006

Healy, M. G., and Hickey, K. R. (2002). Historic land reclamation in the intertidal wetlands of the Shannon estuary, western Ireland. *J. Coast. Res.* 36, 365–373. doi: 10.2112/1551-5036-36.sp1.365

Jia, H., Shen, Y., Su, M., and Yu, C. (2018). Numerical simulation of hydrodynamic and water quality effects of shoreline changes in Bohai Bay. *Front. Earth Sci.* 12, 625-639. doi: 10.1007/s11707-018-0688-x

Kang, J. W. (1999). Changes in tidal characteristics as a result of the construction of Sea-dike/Sea-walls in the mokpo coastal zone in Korea. *Estuarine Coast. Shelf Sci.* 48 (4), 429–438. doi: 10.1006/ecss.1998.0464

Li, F., Ding, D., Chen, Z., Chen, H., Shen, T., Wu, Q., et al. (2020). Change of sea reclamation and the sea-use management policy system in China. *Mar. Policy.* 115, 103861. doi: 10.1016/j.marpol.2020.103861

Li, X., Yuan, D., Sun, J., and Tao, J. H. (2010). "Simulation of land reclamation's effect on the water exchange in tianjin coastal area," in *2010 4th International Conference on Bioinformatics and Biomedical Engineering.* (IEEE), 1–5. doi: 10.1109/icbbe.2010.5517013

Liang, H., Kuang, C., Olabarrieta, M., Song, H., Ma, Y., Dong, Z., et al. (2018). Morphodynamic responses of caofeidian channel-shoal system to sequential large-scale land reclamation. *Continental Shelf Res.* 165, 12–25. doi: 10.1016/j.csr.2018.06.004

Liu, W.-C., Chen, W.-B., and Hsu, M.-H. (2011). Using a three-dimensional particle-tracking model to estimate the residence time and age of water in a tidal estuary. *Comput. Geosci.* 37 (8), 1148–1161. doi: 10.1016/j.cageo.2010.07.007

Pelling, H. E., Uehara, K., and Green, J. A. M. (2013). The impact of rapid coastline changes and sea level rise on the tides in the bohai Sea, China, j. geophys. *Res. Oceans* 118, 3462–3472. doi: 10.1002/jgrc.20258

Song, D., Wang, X. H., Zhu, X., and Bao, X. (2013). Modeling studies of the far-field effects of tidal flat reclamation on tidal dynamics in the East China seas. *Estuarine Coast. Shelf Sci.* 133, 147–160. doi: 10.1016/j.ecss.2013.08.023

Willmott, C. J. (1981). On the validation of models. *Phys. Geogr.* 2, 184. doi: 10.1080/02723646.1981.10642213

Ying, C., Li, R., Li, X., and Liu, Y. (2018). Anthropogenic influences on the tidal prism and water exchange in yueqing bay, zhejiang, China. *J. Coast. Res.* 85, 961–965. doi: 10.2112/si85-193.1

Yuan, Y., Jalón-Rojas, I., and Wang, X. H. (2021). Response of water-exchange capacity to human interventions in jiaozhou bay, China. *Estuar. Coast. Shelf Sci.* 249, 107088. doi: 10.1016/j.ecss.2020.107088

Zhao, X., and Sun, Q. (2013). Influence of reclamation on hydrodynamic environment in bohai bay. *Advanced Mater. Res.* 726-731, 3262–3265. doi: 10.4028/www.scientific.net/amr.726-731.3262

Zhao, L., Wei, H., and Zhao, J. Z. (2002). Numerical study on water exchange in jiaozhou bay. *Chin. J. Oceanol. Limnol.* 33, 23–29.

Zhu, L., Hu, R., Zhu, H., Jiang, S., Xu, Y., and Wang, N. (2018). Modeling studies of tidal dynamics and the associated responses to coastline changes in the bohai Sea, China. *Ocean Dynam.* 68, 1625-1648. doi: 10.1007/s10236-018-1212-2

Zhu, Q., Wang, Y. P., Ni, W., Gao, J., Li, M., Yang, L., et al. (2016). Effects of intertidal reclamation on tides and potential environmental risks: a numerical study for the southern huanghe Sea. *Environ. Earth Sci.* 75 (23), 1-17. doi: 10.1007/s12665-016-6275-0